Toxicology and Applied Pharmacology **172,** 140–149 (2001)
doi:10.1006/taap.2001.9144, available online at http://www.idealibrary.com on IDEAL®

Zinc Tetrakis(*N*-methyl-4′-pyridyl) Porphyrinato Is an Effective Inhibitor of Stimulant-Induced Activation of RAW 264.7 Cells

Jihee Lee Kang,*[,1] In Soon Pack,* Su Min Hong,* Hui Su Lee,* Jong Sik Hah,* Wonwoo Nam,† Stephen Leonard,‡ and Vincent Castranova‡

**Department of Physiology, College of Medicine, Division of Cell Biology, Ewha Medical Research Center and †Department of Chemistry, Division of Molecular Life Sciences, Ewha Womans University, Seoul, 158-056, Korea; and ‡Pathology and Physiology Research Branch, Health Effects Laboratory Division, National Institute for Occupational Safety and Health, Morgantown, West Virginia 26505*

Received October 11, 2000; accepted January 31, 2001

Zinc Tetrakis(*N*-methyl-4′-pyridyl) Porphyrinato Is an Effective Inhibitor of Stimulant-Induced Activation of RAW 264.7 Cells. Kang, J. L., Pack, I. S., Hong, S. M., Lee, H. S., Hah, J. S., Nam, W., Leonard, S., and Castranova, V. (2001). *Toxicol. Appl. Pharmacol.* **172, 140–149.**

One proposed mechanism for the development of silica-induced fibrosis is prolonged pulmonary inflammation and lung damage resulting from the secretion of reactive mediators from alveolar macrophages. Metalloporphyrins have antioxidative and antiinflammatory activities. However, the molecular basis for the anti-inflammatory action of zinc tetrakis(*N*-methyl-4′-pyridyl) porphyrinato (ZnTMPyP) has not been elucidated. The objective of this study was to determine whether ZnTMPyP exhibited the ability to inhibit the production of reactive oxygen species (ROS), the activation of NF-κB, or the secretion of IL-1 in RAW 264.7 cells, and whether such inhibitory activity was related to the ROS-scavenging ability of ZnTMPyP. The results indicate that, although ZnTMPyP is not cytotoxic to RAW 264.7 cells, it is a potent inhibitor in ROS production by RAW 264.7 cells in response to various stimulants, such as silica, zymosan, or phorbol myristate acetate. ZnTMPyP is also effective in reducing stimulant-induced DNA-binding activity of NF-κB and silica-induced tyrosine phosphorylation of IκB-α. ZnTMPyP also inhibits LPS-induced IL-1 production. However, ZnTMPyP exhibits relatively weak ability to directly scavenge hyroxyl or superoxide radicals. On the basis of effective concentrations of ZnTMPyP, these results suggest that ZnTMPyP directly acts as an inhibitor of cellular activation in addition to exhibiting an antioxidant effect. Therefore, it is suggested that further studies concerning the effects of ZnTMPyP using *in vivo* oxidative stress models or its effects on the cytotoxic process of human diseases associated with lung inflammation and injury are warranted. In addition, ZnTMPyP may be a useful tool to investigate the molecular mechanisms involved in stimulant-induced signal pathways. © 2001 Academic Press

[1] To whom correspondence should be addressed at Department of Physiology, College of Medicine, Ewha Womans University, 911-1 Mok-6-dong, Yangcheon-ku, Seoul 158-056, Korea. Fax: 82-2-654-4971; E-mail: jihee@mm.ewha.ac.kr.

Key Words: **ZnTMPyP; reactive oxygen species; NF-κB; IL-1; RAW 264.7 cells.**

Inflammatory and interstitial lung disease caused by exposure to silica is the consequence of a cycle of oxidant damage and resultant lung scarring associated with activation of the fibrotic process. Reactive oxygen species (ROS), such as superoxide anion, hydrogen peroxide, hydroxyl radical or singlet oxygen, nitric oxide, inflammatory cytokines, and growth factors appear critical to this pathogenesis (Castranova, 1998).

Nuclear factor kappa B (NF-κB) is an essential transcription factor that controls gene expression of cytokines, chemokines, growth factors, and cell adhesion molecules that are involved in immune reactions, inflammation, and the control of cell death or transformation (Barnes and Karin, 1997; Baldwin, 1996; Chen *et al.*, 1999). Recent evidence indicates that *in vitro* exposure of RAW 264.7 cells to silica or LPS induces activation of NF-κB (Chen *et al.*, 1998; Kang *et al.*, 2000a). Activation of NF-κB in pulmonary phagocytes has also been demonstrated after *in vivo* exposure to silica (Sacks *et al.*, 1998). Therefore, activation of NF-κB binding to various gene promoter regions appears to be a key molecular event in the initiation of silica-induced pulmonary disease.

The most predominantly characterized NF-κB complex is a p50–p65 heterodimer, which at rest is retained in the cytoplasm and is associated with an inhibitor molecule, IκB (Zabel and Baeuerle, 1990). In response to a variety of stimuli, IκB is phosphorylated and proteolytically degraded or processed by proteasome and other proteases. In a previous study, we suggested tyrosine phosphorylation of IκB-α represents a proteasome proteolytic activity-independent mechanism for NF-κB activation in silica-stimulated RAW 264.7 cells (Kang *et al.*, 2000b). Free NF-κB then translocates into the nucleus, where it binds to various gene promoter regions, controlling the expression of various proinflammatory and proliferative agents (Chen *et al.*, 1999).

Exposure of lung phagocytes to silica results in the produc-

0041-008X/01 $35.00

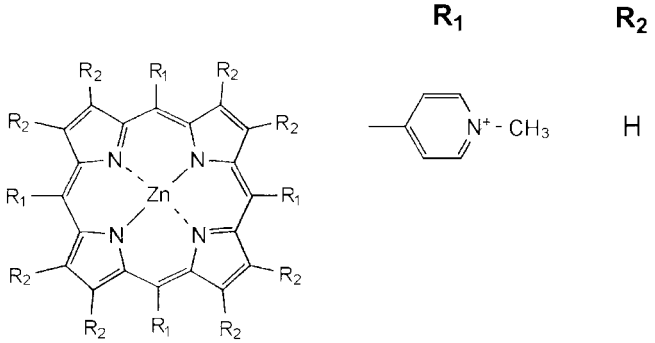

FIG. 1. Chemical structure of ZnTMPyP.

tion of ROS (Castranova *et al.*, 1996), which are believed to be significantly involved in silica-induced cytotoxicity and carcinogenicity (Saffiotti *et al.*, 1985; Vallyathan *et al.*, 1988; Fubini *et al.*, 1990; Castranova, 1994; Shi *et al.*, 1998). Evidence indicates that reactive oxidants play a role in silica-induced activation of NF-κB. Indeed, catalase, superoxide dismutase, and formate have been shown to inhibit silica-induced NF-κB activation of macrophages *in vitro* (Chen *et al.*, 1998; Kang *et al.*, 2000a). Hydroxyl radical has been suggested as the key activation signal for silica-induced activation of NF-κB (Shi *et al.*, 1999).

Zinc tetrakis(*N*-methyl-4′-pyridyl) porphyrinato (ZnTMPyP) is a porphyrin analog having an extensive conjugated ring system that undergoes reversible one-electron oxidation. The structure of ZnTMPyP is given in Fig. 1. Zinc protoporphyrin IX (ZnPP) has antiinflammatory and antiallergic properties (Suyama and Matsumoto, 1964; Suyama *et al.*, 1996a, b; Nagai *et al.*, 1992). ZnPP has also been reported to suppress NO production through a loss of L-arginine (Okada, 1996). Metalloporphyrins, including Fe-, Mn-, and Zn-porphyrins, inhibit heme oxygenase and other heme-dependent enzymes, such as guanylate cyclase and nitric oxide synthase (NOS) (Bashir and Henley, 1993; Luo and Vincent, 1994). ZnPP has been proposed to be the most efficacious brain-protective agent as an IL-1 antagonist or as an inhibitor of these heme-dependent enzymes (Zhao *et al.*, 1996). Recently, Zn-porphyrin has been shown to inhibit the peroxinitrite-induced oxidation and the suppression of mitochondrial respiration by peroxinitrite in cultured J774 macrophages (Zingarelli *et al.*, 1997). However, the effects of ZnTMPyP on *in vitro* or *in vivo* oxidative stress models or cytotoxic processes involved in the development of lung diseases have not been investigated.

The objective of the present investigation was to determine if ZnTMPyP exhibited the ability to inhibit the secretion of reactive oxygen species, the activation of NF-κB, or the production of IL-1 in stimulated RAW 264.7 macrophages and whether such inhibitory activity was related to the ROS-scavenging ability of ZnTMPyP.

METHODS

Reagents. Crystalline silica (Min-U-Sil, particle size <5 μm) was obtained from U.S. Silica Corporation (Berkeley Springs, WV). Prior to use, the silica samples were sterilized by heating at 160°C for 90 min in a dry oven. Silica particles were dispersed in DMEM (Life Technologies, Inc., Madison, WI) with supplements just before addition to culture plates. Lipopolysaccharide (LPS) from *Escherichia coli* serotype 055B5 was purchased from Sigma Chemical Company (St. Louis, MO). ZnTMPyP was purchased from MidCentury (Posen, IL). DNA polymerase and dNTP were purchased from Life Technologies (Gaithersburg, MD). Antibodies used in this study were anti-IκB-α rabbit polyclonal (New England Biolabs, Inc., Bevery, MA) and anti-phosphotyrosine 4G10 (Upstate Biotechnology, Lake Placid, NY).

Cell line and cell culture. RAW 264.7 cells, a mouse peritoneal macrophage cell line, were obtained from American Type Culture Collection (Rockville, MD). The cells were maintained in DMEM (Life Technologies) supplemented with 5% fetal bovine serum (FBS) (HyClone, Logan, UT), 2 mM glutamine, and 1000 units/ml penicillin–streptomycin.

Measurement of cell viability. Lactate dehydrogenase (LDH) is an abundant intracellular enzyme and its release into cell culture supernatants is a marker of lytic cell death (Lipton *et al.*, 1993). The activity of LDH was measured using a LDH determination kit (Roche Molecular Biochemicals, Mannheim, Germany). Briefly, 100 μl of ZnTMPyP (1–100 μM) was added to 100 μl of adherent RAW 264.7 cells (10^4/ml) in given wells of a microplate. The cells were then incubated at 37°C in a humidified atmosphere of 5% CO_2 for 24 h. After incubation, 100 μl of supernatant was added to 100 μl of reaction mixture and incubated for 30 min at room temperature. Absorbency of the samples at 490 nm was measured using a microplate reader. Results were expressed as percent cell viability, referenced to the maximum LDH released when cells were lysed with detergent, using the formula % viability = 100 × (1 − [(experimental − untreated)/(detergent − untreated)]).

Measurement of CL generation. ROS production by RAW 264.7 cells in response to stimulants was determined by measuring cellular chemiluminescence using a luminometer (Berthold, model LB9505AT, Wildbad, Germany). Briefly, cells were washed once with phosphate-buffered saline (145 mM NaCl, 5 mM KCl, 1.9 mM NaH_2PO_4, 9.35 mM Na_2HPO_4, and 5.5 mM glucose, pH 7.4), centrifuged at 500*g* and 4°C for 5 min, and resuspended in Hepes-buffered medium (145 mM NaCl, 5 mM KCl, 10 mM Na Hepes, 5.5 mM glucose, and 1 mM $CaCl_2$, pH 7.4). Cell counts were determined using an electronic cell counter equipped with a cell-sizing attachment (Coulter Electronics, Hialeah, FL).

RAW 264.7 cells (2×10^6 cells/ml) were preincubated for 10 min at 37°C in a shaking water bath and then stimulated with silica (1 mg/ml), zymosan (2 mg/ml), or phorbol 12-myristate 13-acetate (PMA, 3×10^{-6} M) in the presence or absence of ZnTMPyP (1–100 μM). Chemiluminescence was monitored continuously at 37°C for 10 min in the presence of 8 μg% luminol. The integral of cpm versus time was used to compare the total CL between samples.

Nuclear extracts. Nuclear extracts were prepared by a modified method of Sun *et al.* (1994). RAW 264.7 cells were cultured in six-well plates at 5×10^6 cells/ml for 3 days, and then the medium was replaced with fresh medium and cells pretreated with ZnTMPyP (1–100 μM). After a 2-h pretreatment, cells were cultured with silica (100 μg/ml), LPS (1.0 μg/ml), or H_2O_2 (1 mM) in the absence or presence of ZnTMPyP for a period of time as indicated. The concentrations of the stimulants and the duration of exposure used in this investigation were determined from previous concentration–response and time-course studies for NF-κB activation (Kang *et al.*, 2000a). At the end of the exposure, the cells were harvested and resuspended in hypotonic buffer A (100 mM Hepes, pH 7.9; 10 mM KCl; 0.1 M EDTA; 0.5 mM dithiothreitol; 1% nonidet P-40; and 0.5 mM phenylmethylsulfonyl fluoride (PMSF)) for 10 min on ice and then vortexed for 10 s. Nuclei were pelleted by centrifugation at 12,000*g* for 30 s and were resuspended in buffer C (20 mM Hepes, pH 7.9; 20% glycerol; 0.42 M NaCl; 1 mM EDTA; and 0.5 mM PMSF) for 30 min on

ice. The supernates containing nuclear proteins were collected by centrifugation at 10,000*g* for 2 min and stored at −70°C.

Electrophoretic mobility shift assay (EMSA). Binding reaction mixtures (10 μl), containing 5 μg (4 μl) of nuclear extract protein, 2 μg of poly(dI-dC)·poly(dI-dC) (Sigma Co.) and 40,000 cpm of ^{32}P-labeled probe in binding buffer (4 mM Hepes, pH 7.9; 1 mM $MgCl_2$; 0.5 mM DTT; 2% glycerol; and 20 mM NaCl), were incubated for 30 min at room temperature. Protein–DNA complexes were separated on 5% nondenaturing polyacrylamide gels in 1× Tris-borate/EDTA electrophoresis buffer and autoradiographed overnight. Autoradiographic signals for activated NF-κB were quantitated by densitometric scanning using an UltroScan XL laser densitometer (LKB, Model 2222-020, Bromma, Sweden) to determine the intensity of each band.

The oligonucleotide used as a probe for EMSA was a double-stranded DNA containing NF-κB consensus sequence (5′-CCTGTGCTCCGGGAATTTCCCTGGCC-3′) labeled with [α-^{32}P]dATP (Amersham, Buckinghamshire, UK) using a DNA polymerase Klenow fragment.

Immunoprecipitation. The confluent cells grown on 100-mm plastic dishes were incubated in DMEM supplemented with 5% FBS, 2 mM glutamine, and 1000 units/ml penicillin–streptomycin for 3 days. Cells then were treated with silica (100 μg/ml) in the presence or absence of ZnTMPyP (10 μM) and washed with ice-cold phosphate-buffered saline (pH 7.4). The washed cells were lysed with 1 ml of ice-cold lysis buffer containing 50 mM Tris–HCl (pH 8), 150 mM NaCl, 1% nonidet P-40 (NP-40), 100 μg/ml PMSF, 1 μg/ml leupeptin, 1 mM Na_3VO_4, 5 mM EDTA, and 1 mM benzamidine.

The cell lysate was centrifuged for 5 min at 13,000*g*. The resulting supernatant was incubated with anti-IκB-α rabbit polyclonal at 4°C for 1 h. After incubation at 4°C for 30 min with protein A- or G-conjugated sepharose (5 μg/ml), the antigen/antibody complexes were pelleted by centrifugation for 30 s. The pellet was then washed three times with ice-cold lysis buffer by centrifugation at 13,000*g* for 30 s, dissolved in 20 μl of Laemmli's sample buffer, and separated on 10% SDS–polyacrylamide gels (Laemmli, 1970).

Western blotting. The fractionated proteins for tyrosine phosphorylated IκB-α were resolved on 10% SDS–polyacrylamide gels and electrophoretically transferred onto nitrocellulose paper as described by Towbin *et al.* (1979). Antibody labeling of protein bands was detected with enhanced chemiluminescence (ECL) reagents according to the supplier's protocol.

Measurement of IL-1 activity in cultured RAW 264.7 cells. Cells were resuspended in RPMI 1640 media (Mediatech, Washington, DC) containing 2 mM glutamine, 100 units/ml mycostatin, and 10% FBS. Aliquots of 1 ml, containing 10^6 RAW 264.7 cells, were added to 24-well plates (Costar, Cambridge, MA) and incubated at 37°C in a humidified atmosphere of 5% CO_2 for 2 h. The nonadherent cells were then removed by vigorously washing twice with 1 ml of RPMI media. The adherent cells were further incubated in 1 ml of RPMI media containing 5 μg/ml LPS with or without ZnTMPyP in the concentration range of 1–100 μM. After incubating the cell culture for 24 h, the supernates were collected, filtered, and stored at −70°C until the thymocyte proliferation assay was performed.

Thymocyte proliferation assay for IL-1 activity. IL-1 activity in various macrophage-conditioned supernatants was determined by their capacity to stimulate thymocyte proliferation according to the method of Kang *et al.* (1992). Briefly, thymocytes were obtained from male CD-1 mice (6–10 weeks of age) and suspended in RPMI 1640 media with 2 mM glutamine, 100 units/mL penicillin, 100 μg/mL streptomycin, 100 units/mL mycostatin, 10% FBS, and 2×10^{-5} M mercaptoethanol. Cells were counted using an electronic cell counter and adjusted to a concentration of 10×10^6 cells/mL. An aliquot of 100 μL of the RAW 264.7 cell-conditioned supernatants was added in quadruplicate to 96-well microculture plates, and 100 μL of thymocyte suspension was placed in each well. After 48 h incubation at 37°C in 5% CO_2, the cultures were pulsed for 4–6 h with [^{3}H]thymidine (1.0 μCi/well, activity: 2.0 Ci/mmol, Dupont NEN Products, Boston, MA), and harvested using a cell harvester (Brandle, Gaithersburg, MD). The radioactivity in the collecting glass filter disks was measured using a liquid scintillation counter (Beckman, Fullerton, CA). The levels of IL-1 activity in the tested RAW 264.7 cell supernates were expressed as counts per minute.

Free radical measurements. For detection and identification of short-lived radicals, a spin-trapping method was used. This technique involves the addition-type reaction of a short-lived radical with a diamagnetic compound (spin trap) to form a relatively long-lived free radical product, the so-called spin adduct, which can be studied by conventional electron spin resonance (ESR). The intensity of the spin adduct signal corresponds to the amount of short-lived radicals trapped, and the hyperfine splitting of the spin adduct is generally characteristic of the original, short-lived, trapped radical. This method is specific and sensitive and is considered to be the method of choice for the detection and identification of free radicals.

All ESR measurements were conducted using a Bruker ESP 300E ESR spectrometer and a flat cell assembly. Hyperfine couplings were measured (to 0.1 G) directly from magnetic field separation using potassium tetraperoxochromate (K_3CrO_8) and 1,1-diphenyl-2-picrylhydrazyl (DPPH) as reference standards. The relative radical concentration was estimated by multiplying half of the peak height by $(\Delta H_{pp})^2$, where ΔH_{pp} represents peak-to-peak width. An SPEX 300 program (U. S. EPR, Inc. Clarksville, MD) was used for data acquisition and analysis. All experiments were performed at room temperature and under ambient air. Reactants were mixed in test tubes in a final volume of 1.0 ml. The reaction mixture was then transferred to a flat cell for ESR measurement. The concentrations given in the figure legends are final concentrations.

Statistics. Values were expressed as means ± standard errors. Data were analyzed using one way analysis and Student's *t* test. Significance was set at $p < 0.05$.

RESULTS

ZnTMPyP Does Not Affect Cell Viability at Rest

It was essential to demonstrate that ZnTMPyP was not cytotoxic under the conditions used for the functional assays employed in this study. Viability of RAW 264.7 cells was not compromised after a 24-h *in vitro* exposure to ZnTMPyP (1–100 μM), i.e., ZnTMPyP did not increase the activity of LDH in the acellular culture media (data not shown).

ZnTMPyP Inhibits Stimulant-Induced Secretion of ROS

Since ZnTMPyP was not cytotoxic to RAW 264.7 cells, it was possible to determine if ZnTMPyP specifically inhibited the ability of stimulants to activate RAW 264.7 cells. The ability of drug treatment to inhibit the secretion of ROS by RAW 264.7 cells in response to various stimulants was determined by measuring the generation of chemiluminescence (Fig. 2). Particles, such as silica and zymosan, enhanced chemiluminescence generated by RAW 264.7 cells by 2.0- and 2.5-fold, respectively. ZnTMPyP (50 μM) inhibited chemiluminescence generated by silica or zymosan by 100 or 92%, respectively. In addition, while PMA increased chemiluminescence generation by RAW 264.7 cells by 170-fold, there was a 68% decrease of this chemiluminescence after ZnTMPyP (50 μM) treatment. No change of the chemiluminescence was noted in unstimulated cells treated with ZnTMPyP alone. As shown in Fig. 3, ZnTMPyP inhibited silica-stimulated chemiluminescence in a dose-dependent manner with an ID50 of approximately 1 μM and 100% inhibition at 10 μM.

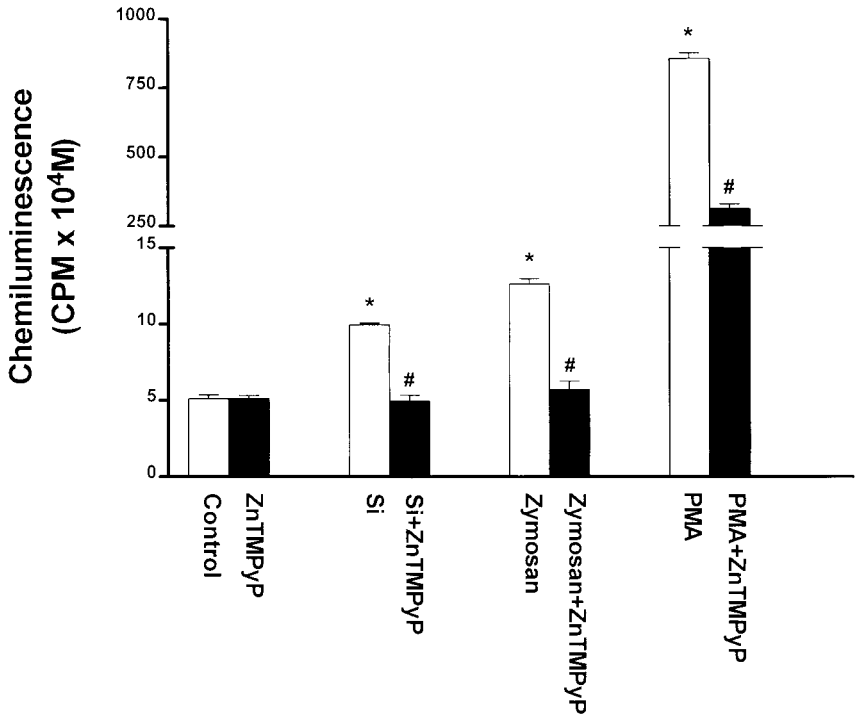

FIG. 2. Effect of ZnTMPyP on chemiluminescence generated by RAW 264.7 cells stimulated with various stimulants. The cells (2×10^6/ml) were preincubated at 37°C for 10 min and then stimulated with silica (1 mg/ml), zymosan (2 mg/ml), or phorbol 12-myristate 13-acetate (PMA, 3×10^{-6} M) in the presence or absence of ZnTMPyP (50 μM). Chemiluminescence was expressed as the integral of cpm versus time. Values are means ± SE of six separate experiments. * Increase from unstimulated cells (control); # Significant decrease compared to each stimulant alone ($p < 0.05$).

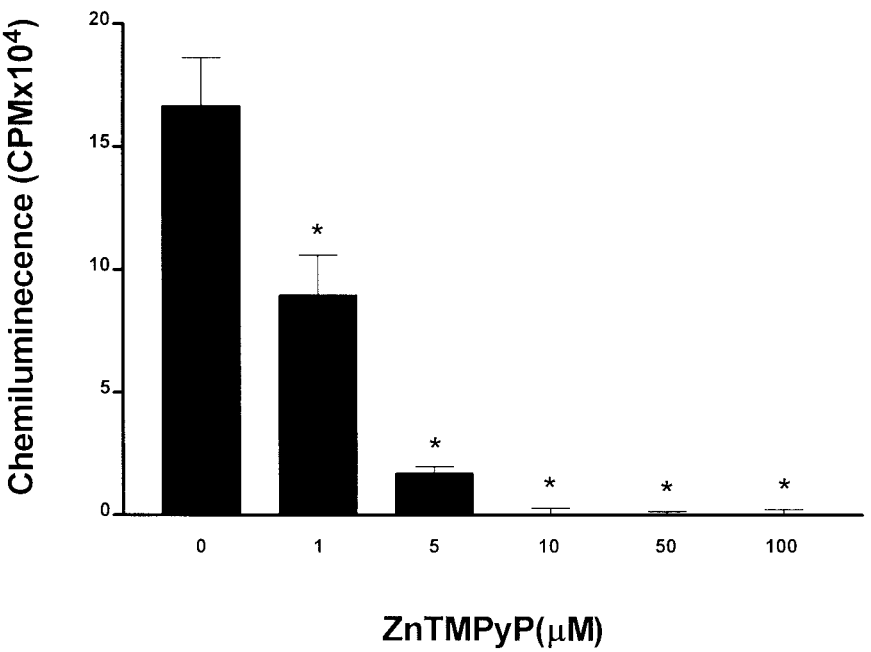

FIG. 3. Effect of ZnTMPyP on chemiluminescence generated by silica-stimulated RAW 264.7 cells. The cells (2×10^6/ml) were preincubated at 37°C for 10 min and then stimulated with silica (1 mg/ml) in the presence or absence of ZnTMPyP (1–100 μM). Chemiluminescence was expressed as the integral of cpm versus time minus that generated from resting cells. Values are means ± SE of six separate experiments. * Significant decrease ($p < 0.05$) compared to silica alone.

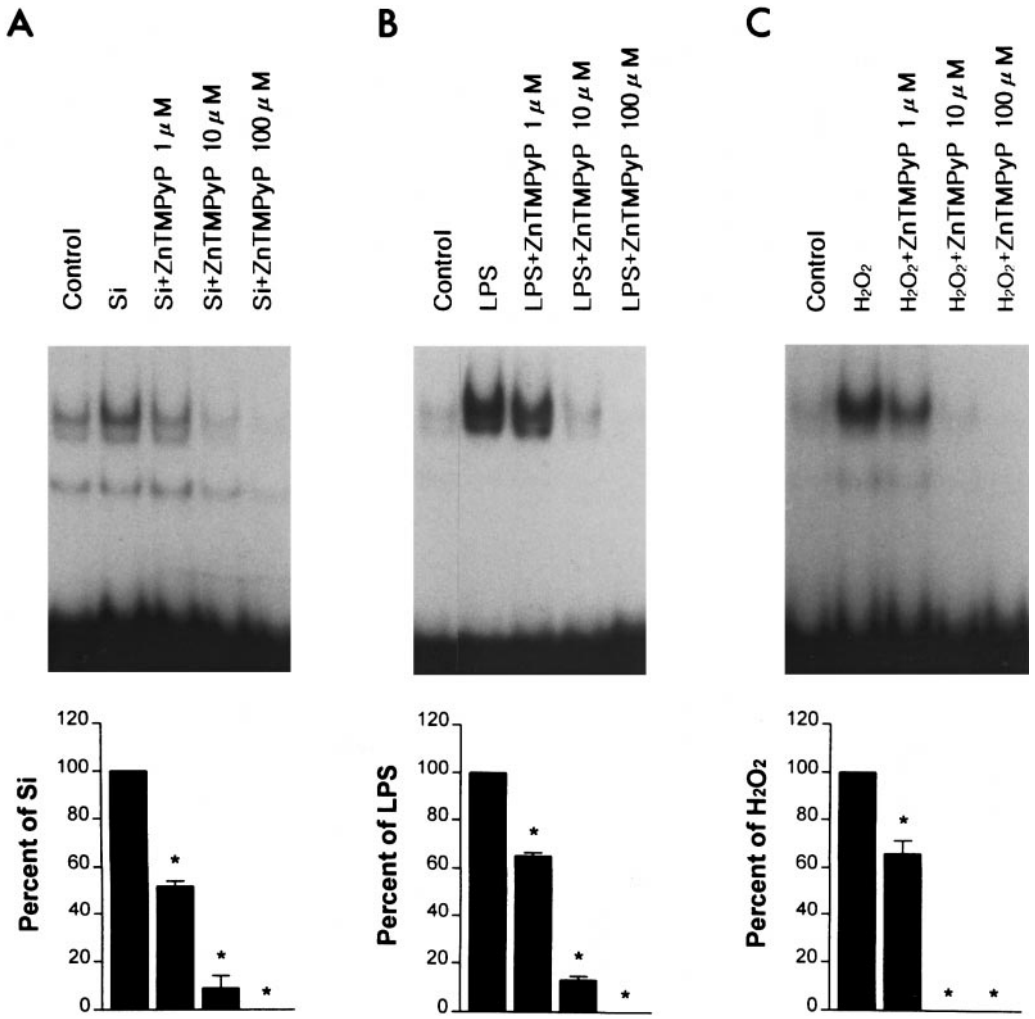

FIG. 4. EMSA illustrating the effect of ZnTMPyP on silica (A)-, LPS (B)-, or H_2O_2 (C)-induced activation of NF-κB. Nuclear extracts were prepared from RAW 264.7 cells pretreated for 2 h with ZnTMPyP (1–100 μM) and then stimulated with silica (100 μg/ml), LPS (10 μg/ml), or H_2O_2 (1 mM) for an additional 4 h. The results of EMSA are shown (top) and quantitated by densitometric analysis as a percentage of the response to stimulant alone minus control (bottom). Values are means ± SE of three separate experiments. * Significant inhibition by ZnTMPyP compared to stimulant alone ($p < 0.05$).

ZnTMPyP Inhibits Stimulant-Induced NF-κB Activation

Since ZnTMPyP completely inhibited oxidant production measured as chemiluminescence in silica-stimulated RAW 264.7 cells, a question is raised as to whether this drug would inhibit NF-κB activation induced by silica. To examine this question, RAW 264.7 cells were preincubated for 2 h with different concentrations of ZnTMPyP and then examined for NF-κB activation by treatment of cells with silica (100 μg/ml) for 4 h at 37°C. ZnTMPyP inhibited the silica-induced binding activity of NF-κB to DNA in a dose-dependent manner with maximum inhibition of 100% at 100 μM (Fig. 4A).

NF-κB activation is also induced by LPS or hydrogen peroxide (Meyer *et al.*, 1993; Chen *et al.*, 1998; Kang *et al.*, 2000a). However, the initial signal transduction pathway leading to NF-κB activation induced by these stimulants has been shown to be different. We, therefore, examined the effect of ZnTMPyP on the activation of NF-κB by these stimulants. The data shown in Figs. 4B and 4C indicate that ZnTMPyP completely blocked the activation of NF-κB induced by LPS at 100 μM or H_2O_2 at 10 μM ZnTMPyP, respectively. These results suggest that ZnTMPyP may act at a common step in the signal transduction pathways leading to NF-κB activation in response to each of these stimulants.

ZnTMPyP Inhibits Silica-Dependent Tyrosine Phosphorylation of IκB-α

To determine whether the inhibitory action of ZnTMPyP on NF-κB activation was due to an effect on silica-dependent tyrosine phosphorylation of IκB-α, cells were pretreated with ZnTMPyP for 2 h before exposure to silica, and cell lysates from silica-treated cells in the presence or absence of the drug were then exposed to IκB-α-specific antibody followed by

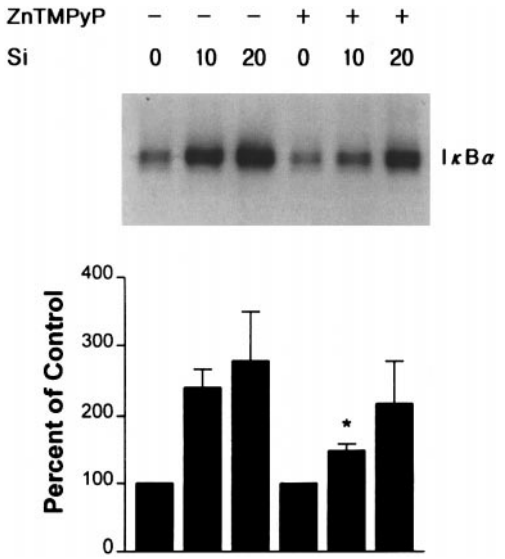

FIG. 5. Effect of ZnTMPyP on silica-dependent tyrosine phosphorylation of IκB-α. RAW 264.7 cells were preincubated for 2 h with ZnTMPyP (10 μM) before treatment with silica (100 μg/ml) for an additional indicated time (10–20 min). The lysates were incubated with anti-IκB-α mAb before analysis of tyrosine phosphorylation by Western blotting with anti-phosphotyrosine mAb (top). The levels of tyrosine phosphorylation IκB-α are quantitated by densitometric analysis as a percentage of the control response (bottom). Values are means ± SE of three separate experiments. * Significant inhibition by ZnTMPyP compared to silica alone at each time of incubation ($p < 0.05$).

Western blot analysis with the anti-phosphotyrosine mAb. ZnTMPyP (10 μM) inhibited tyrosine phosphorylation of IκB-α in cells exposed to silica by 64 and 36% after 10 and 20 min of silica exposure, respectively (Fig. 5). The inhibition of IκB-α phosphorylation after the 10-min silica exposure was statistically significant.

ZnTMPyP Inhibits LPS-Induced IL-1 Production

IL-1 was chosen in our experiments as a representative proinflammatory cytokine because of its prominent role in silica-induced pulmonary inflammatory and fibrotic responses (Kang *et al.,* 1992) and the NF-κB dependence of its gene expression (Baldwin, 1996). To examine the effect of ZnTMPyP on the production of IL-1, we measured thymocyte-proliferation activity in the RAW 264.7 cell supernatants. Evidence indicates that over 90% of this proliferation activity is due to IL-1 (Salem *et al.,* 1990). Figure 6 shows the effect of ZnTMPyP on RAW 264.7 cell production of IL-1 after stimulation by LPS. ZnTMPyP appeared to exert little effect on the resting production of IL-1 from RAW 264.7 cells (data not shown). However, ZnTMPyP inhibited LPS-stimulated IL-1 production from RAW 264.7 cells in a dose-dependent manner, with an ID50 of approximately 10 μM. The maximal inhibition of 88% was exhibited at 100 μM ZnTMPyP. Direct treatment of thymocytes with ZnTMPyP did not affect thymocyte proliferation at rest (data not shown). Therefore, the inhibitory effect described above represents the action of ZnTMPyP directly on the RAW 264.7 cells rather than on the thymocytes.

ZnTMPyP Is a Relatively Weak Antioxidant

To determine the role of ZnTMPyP as a direct antioxidant, its scavenging ability was tested in an hydroxyl radical (·OH)

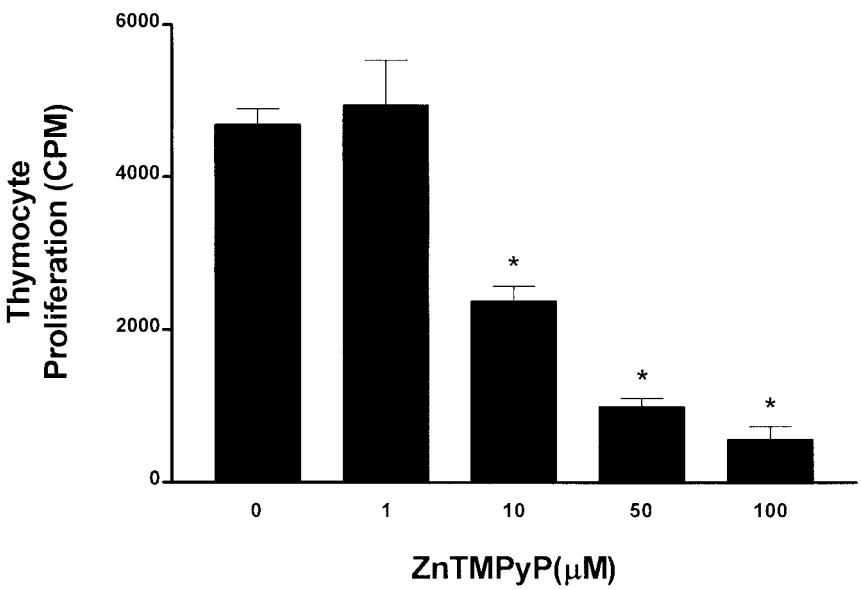

FIG. 6. Effect of ZnTMPyP on IL-1 production from in LPS-stimulated RAW 264.7 cell cultures. RAW 264.7 cells (10^6/ml) were incubated at resting or after stimulation with LPS (5 mg/ml) in the presence or absence of ZnTMPyP (1–100 μM). After 24 h, interleukin-1 (IL-1) activity in the supernatant of cells was measured by thymocyte incorporation of [^{3}H]thymidine. LPS-stimulated IL-1 activity was calculated as cpm minus that with resting cells. Values are means ± SE of three separate experiments. * Significant decrease ($p < 0.05$) compared to LPS alone.

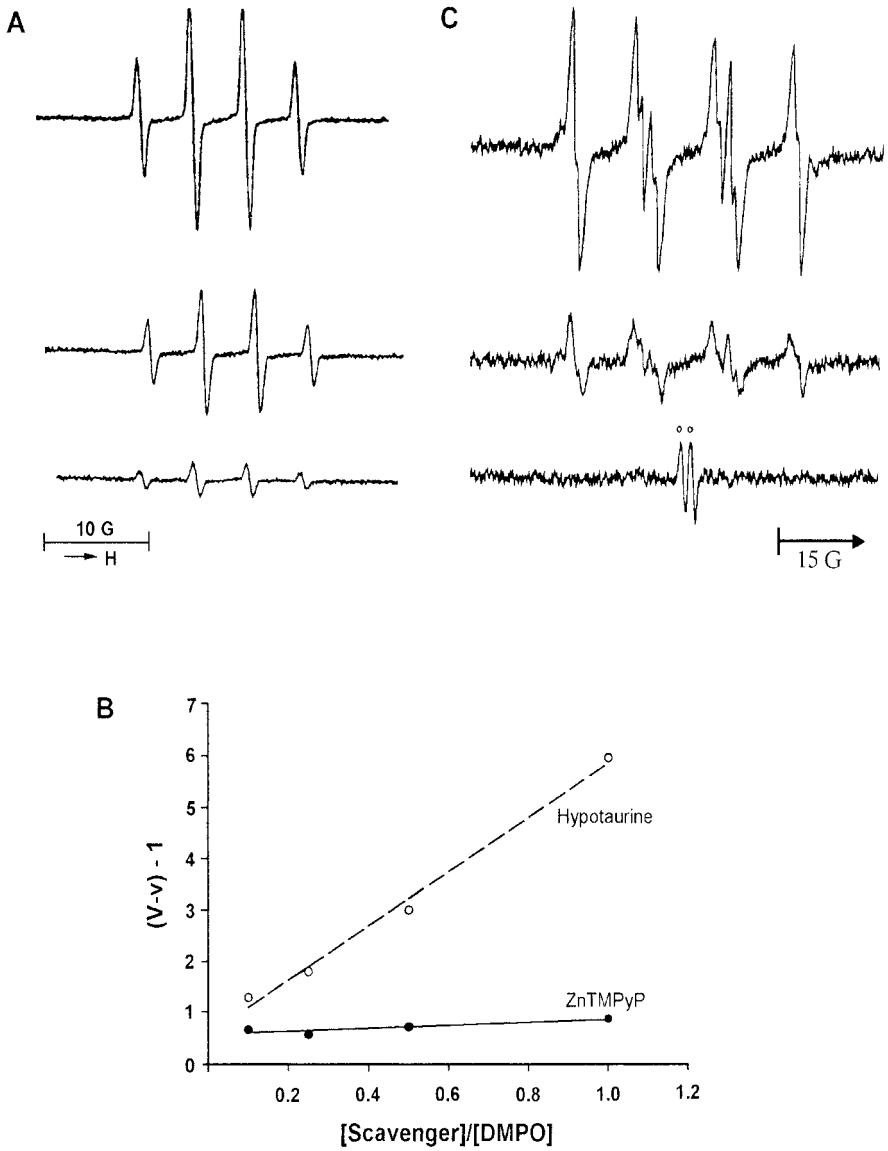

FIG. 7. (A) ZnTMPyP as a hydroxyl radical scavenger. (*Upper signal*) ESR spectrum recorded 2 min after mixing 5 mM $FeSO_4$, 1 mM H_2O_2, and 1 mM DMPO in a pH 7.4 phosphate-buffered solution. (*Middle signal*) Same as *upper signal* but with 100 μM ZnTMPyP added. (*Lower signal*) Same as *uper signal* but with 100 μM hypotaurine added. The spectrum settings were receiver gain, 2.51×10^4; modulation amplitude, 0.5 G; magnetic field, 3435 $\pm$ 50 G; scan time, 1 min.; (B) Scavenging of ·OH by ZnTMPyP or hypotaurine. The ·OH radicals were produced by the reaction of 5 mM $FeSO_4$ with 1 mM H_2O_2 in the presence of 1 mM DMPO. The data were plotted according to equation $(V/v - 1 = k_x[\text{scavenger}]/k_d[\text{DMPO}])$. *V*, Peak height of control = 79.75 mm; *v*, peak height of scavengers. The rate constants of ZnTMPyP and hypotaurine are 1.8×10^9 M^{-1} s^{-1} and 1.24×10^{10} M^{-1} s^{-1}, respectively. (C) Scavenging of O_2^- by ZnTMPyP or ascorbic acid. The O_2^- radicals were produced by the reaction of 3.5 mM xanthine and 2 U xanthine oxidase in the presence of 100 mM DMPO in a pH 7.4 phosphate-buffered solution for 2 min (*upper signal*). *Middle signal* same as *upper signal* but with 100 μM ZnTMPyP added. *Lower signal* same as *upper signal* but with 100 μM ascorbic acid added. The spectrum settings were receiver gain, 2.51×10^4; modulation amplitude, 0.5 G; magnetic field, 3435 $\pm$ 50 G; scan time, 1 min. [circa], ascorbate radicals.

generation system using ESR spectroscopy. Hydroxyl radicals were generated by the Fenton reaction of Fe^{2+} with H_2O_2. Figure 7A (*upper signal*) shows a typical ESR spectrum generated from a mixture containing $FeSO_4$ (5 mM) and H_2O_2 (1 mM) in the presence of DMPO (1 mM) as a spin trap. This spectrum consists of a 1:2:2:1 quarter with splittings of $a_H = a_N = 14.9$ G. Based on these splittings constants, the 1:2:2:1 quartet was assigned to a DMPO/·OH adduct. Addition of ZnTMPyP (100 μM) weakly reduced the ESR signal (Fig. 7A, *middle signal*) in comparison to well established antioxidants, such as hypotaurine (Fig. 7A, *lower signal*) or ascorbate (data not shown).

The reaction rate constant of ZnTMPyP and ·OH radical was calculated through spin-trapping competition experiments as reported earlier (Shi *et al.*, 1997). The rate constant for ZnTMPyP was found to be 1.8×10^9 M^{-1} s^{-1}, which is much less

than hypotaurine (1.24×10^{10} M^{-1} s^{-1}), indicating that the scavenging potency of ZnTMPyP is an order of magnitude lower than that of hypotaurine (Fig. 7B).

To determine the potency of ZnTMPyP as a superoxide anion (O_2^-) scavenger, a xanthine/xanthine oxidase system was used to generate O_2^- and the intensity of this radical monitored by ESR using DMPO as a spin trap. A typical superoxide radical signal is shown in Fig. 7C (*uper signal*). Addition of ZnTMPyP (100 μM) reduced the O_2^- signal by 68% (Fig. 7C, *middle signal*). However, this signal reduction was less than the complete inhibition observed in the presence of 100 μM ascorbic acid (Fig. 7C, *lower signal*).

DISCUSSION

Data presented in this study indicate that ZnTMPyP is an effective *in vitro* inhibitor of stimulant-induced secretion of ROS, NF-κB activation, and IL-1 production in RAW 264.7 cells. These inhibitory actions of ZnTMPyP are not due to cytotoxicity, since ZnTMPyP, at the μM levels used, does not compromise membrane integrity of RAW 264.7 cells. The mechanism by which ZnTMPyP inhibits stimulant-induced activation of RAW 264.7 cells has not yet been resolved.

Patel and Day (1999) have suggested that Zn-porpyrins may be a direct antioxidant, i.e., a scavenger of oxygen radicals. Day *et al.* (1995) have reported ZnTMPyP has activity in the SOD assay even though zinc is not known to alternate between reduction and oxidation states due to a change in valance. One explanation for the SOD-like activity of zinc porphyrins may be due to its ability to undergo reversible one-electron oxidations via its extensive conjugated ring system (Fajer *et al.*, 1970; Wolberg and Manassen, 1970; Dolphin *et al.*, 1971). In fact, the formation of such π-cation catalases and peroxidases has been proposed (Dolphin *et al.*, 1971; Thanabal *et al.*, 1988).

The antioxidant effect of ZnTMPyP is supported by the results of Imai *et al.* (1990), in which metalloporphyrins, including zinc porphyrins and iron porphyrins, were reported to inhibit lipid peroxidation stimulated by Fe^{2+} and ascorbic acid in rat liver homogenates. Their antioxidative effects were not related to the metal ions even if they could be released from the parent porphyrins during incubation. In our experiment, we also found Zn^{2+} had no effect on silica-stimulated secretion of ROS, while TMPyP was an effective inhibitor (data not shown). These results support the conclusion that any antioxidative effect of ZnTMPyP was not brought about by the metal ions. In addition, these results agree with the hypothesis that the antioxidant effect of ZnTMPyP is due to a porphyrin-based mechanism, i.e., reversible one-electron oxidations via its extensive conjugated ring system. However, the porphyrin-based mechanism is probably not as efficient as oxidations that occur on the coordinated metal complex because metalloporphyrins, such as Mn- or Fe-porphyrins, having the ability by reduction and oxidation to change their valance state, are an order of magnitude more active than Zn-porphyrins.

In contrast to the reports above, data from the present study indicate that ZnTMPyP (100 μM) exhibits relatively weak ability to directly scavenge hydroxyl or superoxide radicals, since its potency is much lower than that of well-established antioxidants, such as hypotaurine or ascorbic acid. However, 10 or 50 μM ZnTMPyP completely inhibited silica- or zymosan-stimulated chemiluminescence. In addition, 100 μM ZnTMPyP completely inhibited NF-κB activation induced by various stimulants. These results suggest that, in addition to an antioxidant effect, ZnTMPyP may directly act as an inhibitor of cellular activation.

Nathanson *et al.* (1995) found that Zn-porphyrins suppress the activity of the Na^+/K^+ pump by reduction of the endogenous CO level since Zn-porphyrins are known as potent heme oxygenase inhibitors. Therefore, ZnTMPyP would affect cellular membrane potentials, which may inhibit stimulant-induced activation of RAW 264.7 cells and affect intracellular biochemical homeostasis. However, Miles *et al.* (1981) reported depolarization of alveolar macrophages increased the secretion of ROS. If ZnTMPyP suppressed the activity of the Na/K pump in RAW 264.7 cells, ZnTMPyP would depolarize the cells, which should result in stimulation of ROS secretion. Therefore, the effect of ZnTMPyP on the Na^+/K^+ pump acting as a heme oxygenase inhibitor does not explain the inhibitory effects of ZnTMPyP on stimulant-induced ROS production reported here.

The mechanism in which ZnTMPyP inhibits NF-κB activation is not clear. ROS, protein tyrosine kinase, protein kinase C, protein tyrosine phosphatase, and proteases have been shown to play roles in the activation of NF-κB. As the stimulants employed in this study are known to induce ROS and/or PTK-dependent NF-κB activation in RAW 264.7 cells (Kang *et al.*, 2000a), it is possible that ZnTMPyP exerts its effect by inhibiting ROS secretion and/or preventing PTK activation. This hypothesis is consistent with our finding that ZnTMPyP inhibited stimulant-induced ROS production and protein tyrosine phosphorylation (data not shown).

Data from our previous study indicate that stimulation of RAW 264.7 cells with silica induces NF-κB activation through tyrosine phosphorylation of IκB-α without dependence on degradation of IκB-α (Kang *et al.*, 2000b). The results from the present study show that ZnTMPyP blocks tyrosine phosphorylation of IκB-α in silica-stimulated RAW 264.7 cells. In addition, we found ZnTMPyP also inhibited degradation of IκB-α induced by LPS, which is essential for NF-κB activation (data not shown). Similar effects of ZnTMPyP on tyrosine phosphorylation as well as degradation of IκB-α have been reported with antioxidants and specific inhibitors of PTK (Kang *et al.*, 2000b; Natarajan *et al.*, 1998; Imbert *et al.*, 1998). These findings suggest that ZnTMPyP may act on the step that links reactive oxidants, PTK, and NF-κB activation.

It has been postulated that ROS play a regulatory role in the

protein tyrosine phosphorylation as well as NF-κB activation (Suzuki *et al.*, 1997; Remacle *et al.*, 1995). ROS have also been implicated as important mediators in silica-induced lung injury (Kang *et al.*, 1992) and ROS may serve as mediators of production of cytokines, such as IL-1 and TNFα, in stimulated cells (Simeonova and Luster, 1996; Kawashima *et al.*, 1998). In the present study, increases in NF-κB binding to DNA as well as IL-1 production by LPS-stimulated RAW 264.7 cells were inhibited by ZnTMPyP. However, the effect of this drug on NF-κB-dependent gene expression of IL-1 and the promoter activation specific to IL-1 as well as other cytokines remains to be understood.

In conclusion, our findings indicate that ZnTMPyP is effective in preventing stimulant-induced ROS generation, NF-κB activation, and IL-1 production in RAW 264.7 cells. Therefore, it is suggested that further studies concerning the effects of ZnTMPyP using *in vivo* oxidative stress models or its effects on the cytotoxic process of human diseases associated with lung inflammation and injury are warranted. In addition, ZnTMPyP may be a useful tool to investigate the molecular mechanisms involved in stimulant-induced signal pathways.

ACKNOWLEDGMENT

This work was supported by the National R&D Program (97-NS-01-01-A-13) for Women's Universities.

REFERENCES

Baldwin, A. S., Jr. (1996). The NF-κB and IκB proteins: New discoveries and insights. *Annu. Rev. Immunol.* **14,** 649–683.

Barnes, P. J., and Karin, M. (1997). Nuclear factor-kappa B: A pivotal transcription factor in chronic inflammatory diseases. *N. Engl. J. Med.* **366,** 1066–1071.

Bashir, Z. I., and Henley, J. M. (1993). The French connection: A magnum of excitatory amino acids in Marseilles. *Trends Pharmacol. Sci.* **14,** 387–390.

Castranova, V. (1994). Generation of oxygen radicals and mechanisms of injury prevention. *Environ. Health Perspect.* **102**(Suppl. 10), 65–68.

Castranova, V., Antonini, J. M., Reasor, M. J., Wu, L., and Van Dyke, K. (1996). Oxidant release from pulmonary phagocytes. In (V. Castranova, V. Vallyathan, and W. E. Wallace, Eds.), pp. 185–195. *Silica and Silica-Induced Lung Disease* CRC Press, Boca Raton, FL.

Castranova, V. (1998). Particles and the airways: Basic biological mechanisms of pulmonary pathogenicity. *Appl. Occup. Environ. Hyg.* **13,** 613–616.

Chen, F., Lu, Y., Demers, L. M., Rojanasakul, Y., Shi, X., Vallyathan, V., and Castranova, V. (1998). Role of hydroxyl radical in silica-induced NF-κB activation in macrophages. *Ann. Clin. Lab. Sci.* **28,** 1–13.

Chen, F., Castranova, V., Shi, X., and Demers, L. M. (1999). New insights into the role of nuclear factor-κB, a ubiquitous transcription factor in the initiation of diseases. *Clin. Chem.* **45,** 7–17.

Day, B. J., Shawen, S., Liochev, S. I., and Crapo, J. D. (1995). A metalloporphyrin superoxide dismutase mimetic protects against paraquat-induced endothelial cell injury, in vitro. *J. Pharmacol. Exp. Ther.* **275,** 1227–1232.

Dolphin, D., Forman, A., Borg, D. C., Fajer, J., and Felton, R. H. (1971). Compounds I of catalase and horseradish peroxidase: π-Cation radicals. *Proc. Natl. Acad. Sci. USA* **68,** 614–618.

Fajer, J., Borg, D. C., Forman, A., Dolphin, D., and Felton, R. H. (1970). π-Cation radicals and dications of metalloporphyrins. *J. Am. Chem. Soc.* **92,** 3451–3459.

Fubini, B., Giamello, E., Volante, M., and Bolis, V. (1990). Chemical functionalities at the silica surface determining its reactivity when inhaled. Formation and reactivity of surface radicals. *Toxicol. Ind. Health* **6,** 571–598.

Imai, K., Aimoto, T., Sato, M., and Kimura, R. (1990). Antioxidative effect of several porphyrins on lipid peroxidation in rat liver homogenates. *Chem. Pharm. Bull.* **38,** 258–260.

Imbert, V., Rupec, R. A., Livolsi, A., Pahl, H. L., Traenckner, E. B., Mueller-Dieckmann, C., Farahifar, D., Rossi, B., Auberger, P., Baeuerle, P. A., and Peyron, J. F. (1996). Tyrosine phosphorylation of IκB-α activates NF-κB without proteolytic degradation of IκB-α. *Cell* **86,** 787–798.

Kang, J. H., Lewis, D. M., Castranova, V., Rojanasakul, Y., Banks, D. E., Ma, J. Y., and Ma, J. K. (1992). Inhibitory action of tetrandrine on macrophage production of interleukin-1 (IL-1)-like activity and thymocyte proliferation. *Exp. Lung Res.* **18,** 715–729.

Kang, J. L., Go, Y. H., Hur, K. C., and Castranova, V. (2000a). Silica induced nuclear factor-κB activation: Involvement of reactive oxygen species and protein tyrosine kinase activation. *J. Toxicol. Environ. Health Part A* **60,** 27–46.

Kang, J. L., Pack, I. S., Hong, S. M., Lee, H. S., and Castranova, V. (2000b). Silica induced nuclear factor-κB activation through tyrosine phosphorylation of IκB-α in RAW 264.7 macrophages. *Toxicol. Appl. Pharmacol.* **169,** 59–65.

Kawashima, S., Hayashi, M., Takii, T., Kimura, H., Zhang, H. L., Nagatsu, A., Sakakibara, J., Murata, K., Oomoto, Y., and Onozaki, K. (1998). Serotonin derivative, *N*-(*p*-coumaroyl) serotonin, inhibits the production of TNF-alpha, IL-1 alpha, IL-1 beta, and IL-6 by endotoxin-stimulated human blood monocytes. *J. Interferon Cytokine Res.* **18,** 423–428.

Laemmli, U. K. (1970). Cleavage of structural proteins during the assembly of the head of bacteriophage T4. *Nature* **227,** 680–685.

Lipton, S. A., Choi, Y. B., Pan, Z. H., Lei, S. Z., Chen, H. S., Sucher, N. J., Loscalzo, J., Singel, D. J., and Stamler, J. S. (1993). A redox-based mechanism for the neuroprotective and neurodestructive effects of nitric oxide and related nitroso-compounds. *Nature* **364,** 626–632.

Luo, D., and Vincent, S. R. (1994). Metalloporphyrins inhibit nitric oxide-dependent cGMP formation in vivo. *Eur. J. Pharmacol.* **267,** 263–267.

Meyer, M., Schreck, R., and Baeuerle, P. A. (1993). H_2O_2 and antioxidants have opposite effects on activation of NF-kappaB and AP-1 in intact cells: AP-1 as secondary antioxidant-responsive factor. *EMBO J.* **12,** 2005–2015.

Miles, P. R., Bowman, L., and Castranova, V. (1981). Transmembrane potential changes during phagocytosis in rat alveolar macrophages. *J. Cell. Physiol.* **106,** 109–117.

Nagai, H., Kitagaki, K., Kuwabara, K., and Koda, A. (1992). Anti-inflammatory properties of zinc protoporphyrin disodium(Zn-PP-2Na). *Agents Actions* **37,** 273–283.

Natarajan, K., Manna, S. K., Chaturvedi, M. M., and Aggarwal, B. B. (1998). Protein tyrosine kinase inhibitors block tumor necrosis factor-induced activation of nuclear factor-κB, degradation of IκBα, nuclear translocation of p65, and subsequent gene expression. *Arch. Biochem. Biophys.* **352,** 59–70.

Nathanson, J. A., Scavone, C., Scanlon, C., and McKee, M. (1995). The cellular Na^+ pump as a site of action for carbon monoxide and glutamate: A mechanism for long-term modulation of cellular activity. *Neuron* **14,** 781–794.

Okada, D. (1996). Zinc portoporphyrin IX suppresses nitric oxide production through a loss of L-arginine in rat cerebellar slices. *Neurosci. Res.* **25,** 353–358.

Patel, M., and Day, B. J. (1999). Metalloporphyrin class of therapeutic catalytic antioxidants. *Trends Pharmacol. Sci.* **20,** 359–364.

Remacle, J., Raes, M., Toussaint, O., Renard, P., and Rao, G. (1995). Low

levels of reactive oxygen species as modulators of cell functions. *Mutat. Res.* **316,** 103–122.

Sacks, M., Gordon, J., Bylander, J., Porter, D., Shi, XL., Castranova, V., Kaczmarczyk, W., Van Dyke, K., and Reasor, M. J. (1998). Silica-induced pulmonary inflammation in rats: Activation of NF-kappa B and its suppression by dexamethasone. *Biochem. Biophys. Res. Commun.* **253,** 181–184.

Saffiotti, U., Williams, A. O., Daniel, L. N., Kaighn, M. E., Mao, Y., and Shi, X. (1985). Carcinogenesis by crystalline silica: Animal, cellular, and molecular studies. In (V. Castranova, V. Vallyathan, and W. E. Wallace, Eds.), pp. 345–381. *Silica and Silica-Induced Lung Diseases* CRC Press, Boca Raton, FL.

Salem, P., Deryckx, S., Dulioust, A., Vivier, E., Denizot, Y., Damais, C., Dinnrello, C. A., and Thomas, Y. (1990). Immunoregulatory functions of paf-acether IV. Enhancement of IL-1 production by muramyl dipeptide-stimulated monocytes. *J. Immunol.* **144,** 1338–1344.

Shi, X., Flynn, D. C., Porter, D. W., Leonard, S. S., Vallyathan, V., and Castranova, V. (1997). Efficacy of taurine based compounds as hydroxyl radical scavengers in silica-induced peroxidation. *Ann. Clin. Lab. Sci.* **27,** 365–374.

Shi, X., Castranova, V., Halliwell, B., and Vallyathan, V. (1998). Reactive oxygen species and silica-induced carcinogenesis. *J. Toxicol. Environ Health Part B* **1,** 181–197.

Shi, X., Ding, M., Dong, Z., Chen, F., Ye, J., Wang, S., Leonard, S. S., Castranova, V., and Vallyathan, V. (1999). Antioxidant properties of aspirin: Characterization of the ability of aspirin to inhibit silica-induced lipid peroxidation, DNA damage, NF-κB activation and TNFα production. *Mol. Cell. Biochem.* **199,** 93–102.

Simeonova, P. P., and Luster, M. L. (1996). Asbestos induction of nuclear transcription factors and interleukin 8 gene regulation. *Am. J. Respir. Cell Mol. Biol.* **15,** 787–795.

Sun, S. C., Elwood, J., Beraud, C., and Greene, W. C. (1994). Human T-cell leukemia virus type I Tax activation of NF-kappa B/Rel involves phosphorylation and degradation of I kappa B alpha and RelA (p65)-mediated induction of the *c*-rel gene. *Mol. Cell. Biol.* **14,** 7377–7384.

Suyama, T., and Matsumoto, T. (1964). Anti-inflammatory effects of protoporphyrin (1)—Effects on experimental cirrhosis of the liver, granuloma and euptibility of small-pox vaccine. *Kanazawa-zyuzen igakukai zasshi* **70,** 694–701. [In Japanese]

Suyama, T., Matsumoto, T., and Oguro, Y. (1966a). Anti-inflammatory-effects of protoporphyrin (2)—Effects on hypersensitive reactions, antibody production and immune hemolysis. *Kanazawa-zyuzen igakukai zasshi* **73,** 199–205. [In Japanese]

Suyama, T., Matsumoto, T., and Odashima, S. (1966b). Anti-inflammatory effects of protoporphyrin (3)—Orally administered protoporphyrin: Its effects on experimental liver cirrhosis and on anaphylactic shock. *Kanazawa-zyuzen igakukai zasshi* **74,** 256–270. [In Japanese]

Suzuki, Y. J., Forman, H. J., and Sevanian, A. (1997). Oxidants as stimulators of signal transduction. *Free Radical Biol. Med.* **22,** 269–285.

Thanabal, V., La Mar, G. N., and de Ropp, J. S. (1988). A nuclear overhauser effect study of the heme crevice in the resting state and compound I of horseradish peroxidase: Evidence for cation radical delocalization to the proximal histidine. *Biochemistry* **27,** 5400–5407.

Towbin, H., Staehelin, T., and Gordon, J. (1979). Electrophoretic transfer of proteins from polyacrylamide gels to nitrocellulose sheets: Procedure and some applications. *Proc. Natl. Acad. Sci. USA* **76,** 4350–4354.

Vallyathan, V., Shi, X., Dalal, N. S., Irr, W., and Castranova, V. (1988). Generation of free radical from freshly fractured silica dust. Potential role in acute silica-induced lung injury. *Am. Rev. Respir. Dis.* **138,** 1213–1219.

Wolberg, A., and Manassen, J. (1970). Electrochemical and electron paramagnetic resonance studies of metalloporphyrins and their electrochemical oxidation products. *J. Am. Chem. Soc.* **92,** 2982–2991.

Zabel, U., and Baeuerle, P. A. (1990). Purified human IκB can rapidly dissociate the complex of the NF-κB transcription factor with its cognate DNA. *Cell* **61,** 255–265.

Zhao, Y. J., Yang, G. Y., and Domino, E. F. (1996). Zinc protoporphyrin, zinc ion, and protoporphyrin reduce focal cerebral ischemia. *Stroke* **27,** 2299–2303.

Zingarelli, B., Day, B. J., Crapo, J. D., Salzman, A. L., and Szabo, C. (1997). The potential role of peroxynitrite in the vascular contractile and cellular energetic failure in endotoxic shock. *Br. J. Pharmacol.* **120,** 259–267.